Soil Moisture Effect on Thermal Infrared (8–13-μm) Emissivity

Maria Mira, Enric Valor, Vicente Caselles, Eva Rubio, César Coll, Joan M. Galve, Raquel Niclòs, Juan M. Sánchez, and Rafael Boluda

***Abstract*—Thermal infrared (TIR) emissivities of soils with different textures were measured for several soil moisture (SM) contents under controlled conditions using the Box method and a high-precision multichannel TIR radiometer. The results showed a common increase of emissivity with SM at water contents lower than the field capacity. However, this dependence is negligible for higher water contents. The highest emissivity variations were observed in sandy soils, particularly in the 8–9-μm range due to water adhering to soil grains and decreasing the reflectance in the 8–9-μm quartz doublet region. Thus, in order to model the emissivity dependence on soil water content, different approaches were studied according to the *a priori* soil information. Soil-specific relationships were provided for each soil texture and different spectral bands between 8 and 13 μm, with determination coefficients up to 0.99, and standard estimation errors in emissivity lower than $\pm$0.014. When considering a general relationship for all soil types, standard estimation errors up to $\pm$0.03 were obtained. However, if other soil properties (i.e., organic matter, quartz, and carbonate contents) were considered, along with soil water content, the general relationship predicted TIR emissivities with a standard estimation error of less than $\pm$0.008. Furthermore, the study showed the possibility of retrieving SM from TIR emissivities with a standard estimation error of about $\pm 0.08\ \mathrm{m^3 \cdot m^{-3}}$.**

***Index Terms*—Emission, infrared measurements, modeling, moisture, remote sensing, soil.**

Manuscript received May 29, 2009; revised November 25, 2009. First published February 5, 2010; current version published April 21, 2010. This work was carried out at the University of Valencia, Spain, and was supported in part by the Spanish Ministry of Science and Innovation (Research Grants of M. Mira and J. M. Galve; Juan de la Cierva Contracts of R. Niclòs and J. M. Sánchez; Projects CGL2007-64666/CLI, CGL2007-29819-E/CLI, CGL2007-28828-E/BOS, and CGL2006-0976, which are cofinanced by FEDER funds), by the Generalitat Valenciana (PROMETEO/2009/086), and by the European Space Agency (SMOS Cat-1 Project AO-4748).

M. Mira, E. Valor, V. Caselles, C. Coll, and J. M. Galve are with the Department of Earth Physics and Thermodynamics, Faculty of Physics, University of Valencia, 46100 Burjassot, Spain (e-mail: maria.mira@uv.es).

E. Rubio is with the Department of Applied Physics, School of Industrial Engineering of Albacete (EIIAB), University of Castilla-La Mancha, 02071 Albacete, Spain, and also with the Institute of Regional Development, University of Castilla-La Mancha, 02071 Albacete, Spain.

R. Niclòs is with the Fundación Centro de Estudios Ambientales del Mediterráneo (CEAM), 46980 Paterna, Spain.

J. M. Sánchez is with the Department of Applied Physics, School of Industrial Engineering of Albacete (EIIAB), University of Castilla-La Mancha, 02071 Albacete, Spain, and also with the Department of Earth Physics and Thermodynamics, Faculty of Physics, University of Valencia, 46100 Burjassot, Spain.

R. Boluda is with the Department of Vegetal Biology, Faculty of Pharmacy, University of Valencia, 46100 Burjassot, Spain.

Color versions of one or more of the figures in this paper are available online at http://ieeexplore.ieee.org.

Digital Object Identifier 10.1109/TGRS.2009.2039143

I. Introduction

SURFACE emissivity is a key parameter for determining long-wave surface energy balance, which is strongly influenced by the difference between land surface temperature (LST) and sky brightness temperature. This difference can be neglected outside the 7–14-μm atmospheric window region where the change in the emitted radiation caused by emissivity variability is mostly compensated by changes in the reflected sky radiance. However, this difference becomes relevant within the atmospheric window due to the low sky brightness. Because of the relative transparency of the atmosphere at these wavelengths, it is possible to estimate LSTs and emissivities from multispectral thermal infrared (TIR) remote sensing [1]–[3]. In addition, knowledge of the emissivity spectrum is useful to map geologic and land-cover materials based on differences in wavelength-dependent spectral features [4]–[7].

The influence of soil texture on emissivity is well known from experimental studies [4]–[10]. However, up to now, few published works analyze the soil moisture (SM) effect on thermal emissivities [11]–[13]. Mira *et al.* [14] recently assessed the importance of an accurate determination of the TIR emissivity variation with soil water content to permit accurate temperature retrievals. The study showed systematic errors from 0.1 to 2 K due to SM influence on emissivity. In [14], TIR (8–13-μm) emissivities of six soil samples with different textures were measured under controlled SM content in order to obtain quantitative relationships between SM and spectral emissivities. The best determination coefficients ($R^2 \sim 0.90$ on average) were achieved when using specific equations for each spectral band and soil sample, using a quadratic function of emissivity with SM. The measurements showed an emissivity increase up to 0.16 when water content increased by 24% in the 8.2–9.2-μm region, with the larger increases at low water contents and high sand contents. It is worth noting that the high content of sand particle in the soil favors a lower content of organic matter (OM) since sand texture conditions its mineralization, but not the gain of soil water retention capacity. It is the purpose of this paper to complete the work presented in [14] by providing the results of emissivity variation with SM for an additional set of eight new soil samples of different textures, in order to obtain a general relationship to define the SM dependence of thermal emissivities of soils. Furthermore, the possibility of retrieving SM estimates from TIR emissivities is analyzed.

This paper proceeds as follows. The next section provides a description of the soil samples, the measurement of volumetric water contents, and the measurement of TIR emissivities by means of the Box method. The results of the experiment are

TABLE I
SOIL SAMPLE PROPERTIES, INCLUDING LOCATION, SOIL TEXTURE, BULK MINERALOGY, AND SOIL WATER CHARACTERISTIC ESTIMATES BY TEXTURE AND OM FOLLOWING SAXTON AND RAWLS [36]. FC: FIELD CAPACITY; WP: WILTING POINT MOISTURE

	Samples							
	WS	LW03	LW13	LW45	LW52	BR1	BR2	BR3
Location	32°49'26''N 106°16'23''W	34°57'51"N 98°4'34"W	34°55'16"N 97°57'11"W	34°55'37"N 98°18'14"W	34°47'49"N 98°6'54"W	21°57'43"S 47°50'34"W	22°56'11"S 47°43'24"W	22°45'18"S 47°53' 75"W
Color, dry	7.5Y8/1	7.5YR7/3	10YR5/6	2.5Y6/8	5YR7/4	5YR6/3	2.5Y6/3	7.5YR6/4
Color, wet	7.5Y8/1	10YR6/3	10YR6/3	7.5YR5/1	10YR5/4	7.5YR6/6	7.5YR5/6	5Y5/6
pH (H_2O)	9.01 ± 0.19	7.14 ± 0.09	7.53 ± 0.12	4.70 ± 0.08	6.70 ± 0.09	4.3 ± 0.2	5.3 ± 0.2	3.8 ± 0.2
OM, %	0.21	0.73 ± 0.04	1.61 ± 0.09	1.15 ± 0.08	1.71 ± 0.10	2.93 ± 0.08	1.47 ± 0.09	1.69 ± 0.10
$CaCO_3$, %	0.0	0.0	0.0	0.0	0.0	0.0	0.0	0.0
Sand, %	100.0	77.2	50.8	29.2	62.4	40	69	92
Silt, %	0.0	17.6	35.6	53.6	15.2	6	15	2
Clay, %	0.0	5.2	13.6	17.2	22.4	54	16	6
Texture	sand	loamy sand	loam	silty loam	sandy clay loam	clay	sandy loam	sand
Gypsum, %	99	-	-	-	-	-	-	-
Quartz, %	1	53.7	76.0	72.4	58.4	37.9	82.3	100.0
Feldspar, %	-	46.3	16.7	23.4	32.2	-	16.8	-
Phyllosilicate, %	-	-	4.8	4.2	9.4	-	0.8	-
Gibbsite, %	-	-	-	-	-	49.0	-	-
Hematite, %	-	-	2.6	-	-	13.1	-	-
Bulk density, g cm^{-3}	2.10	1.68	1.48	1.41	1.43	1.22	1.43	1.45
WP, cm^3cm^{-3}	0.002	0.033	0.097	0.112	0.143	0.324	0.107	0.047
FC, cm^3cm^{-3}	0.036	0.101	0.218	0.276	0.238	0.438	0.189	0.088
Saturation, cm^3cm^{-3}	0.425	0.411	0.428	0.429	0.419	0.469	0.416	0.442

described and analyzed in Section III, and finally, the main conclusions are given in Section IV.

II. EXPERIMENTAL SETUP

A. Soil Sample Description

We selected eight soil samples with a diversity of soil types that complement the previous work by Mira *et al.* [14]. They included one sample from the 710-km^2 White Sands National Monument in New Mexico, U.S. (labeled as WS), four soils sampled in the 610-km^2 Little Washita River Experimental Watershed (LWREW) in south central Oklahoma, U.S. (labeled as LW03, LW13, LW45, and LW52, following the identification name of the 2.6-km^2 sampling fields within the LWREW), and three soils from a rural area in São Paulo, Brazil (labeled as BR1, BR2, and BR3). The samples were taken from the upper 15 cm of the A horizon, designated as the *top layer* and characteristic for being the layer that is darker in color than deeper layers and the mineral soil with most OM accumulation and biological activity. The main properties of the soils are presented in Table I. The identification of clay minerals was determined by means of the X-ray diffraction technique and a semiquantitative analysis of the patterns following the methods described in [15]–[17]. The soil composition for these sites ranged from 29% to 100% for sand, 0% to 54% for clay, 0.2% to 2.9% for OM, and 1% to 100% for quartz, while no soil contained carbonate. Quartz abundance in most samples is highlighted here due to the low emissivity values at the quartz Reststrahlen bands around 7.7, 9.7, and near 12.6 μm [4].

B. SM Measurement

The measurement strategy and the configuration details of the container designed to keep the soils and allow water drainage and a practical execution of emissivity measurements are given in [14]. In that study, the gravimetric method was chosen for measuring the SM, since it is considered the most accurate technique. However, it is a laborious and destructive method since small amounts of soil are removed from the total sample when SM measurements are done. For these reasons and because models usually require volumetric SM, which implies less precisely measured densities, we calculated volumetric SM measurements using time-domain reflectometry (TDR) [18], [19] in this study. Volumetric SM is defined as the ratio of the volume of water contained to the total volume of the soil sample and can be obtained from gravimetric SM by considering the bulk density of the sample.

The high dielectric constant or relative permittivity of water ($\kappa \sim 80$) compared to that of the other soil components ($\kappa \sim 1$ for air and $\kappa \sim 2$ to 5 for soils) makes the determination of relative permittivity a suitable way to measure water content. This is the base of the TDR, which is a radar technique applied within the soil. TDR has improved our ability to characterize simultaneously and very accurately the storage and movement of soil water, ionic solutes, and air (indirectly) in the soil profile in both space and time, with relatively low equipment and labor costs. In TDR, a fast-rise step voltage pulse is propagated along a transmission line in the soil. The voltage pulse propagates as an electromagnetic wave, which travels in the soil and is guided by the conductors of a probe (metal rods). The measurement of its propagation velocity (or time delay) and attenuation are used to determine volumetric soil water content, since the ratio of the TDR travel time in soil to that measured in air, i.e., t/t_{air}, is equivalent to $\kappa^{1/2}$.

An empirical relationship between relative permittivity κ and volumetric water content θ_v, namely, the "Topp equation" [18], was initially used for conversion of TDR data to θ_v. Later improvements and refinements have made use of the dielectric mixing formulas that require an additional prior knowledge of the soil properties, such as density, texture, and/or OM content [20], [21]. However, from the analyses by Topp and Reynolds [19] and the related experimental work [21], it has been shown

that the relationship between $\kappa^{1/2}$ and θ_v is linear over what can be considered a practical range of water content.

In our experiment, the SM sensor Delta-T SM200 was used, which has a calibration uncertainty of ± 0.03 $\mathrm{m}^3 \cdot \mathrm{m}^{-3}$ for θ_v determinations according to the manufacturers [22]. The SM200 sensor is most sensitive to signals very close to the two rods, but a small proportion of the signal reaches up to 50 mm from the rods. This is why SM measurements were always made at least 100 mm far from the box edges, to avoid the influence of the box on the TDR response. Because of the wide range of soil textures for our samples, it was necessary to determine the effects of using a generalized factory-supplied calibration on the determination of soil water content from TDR time delay readings. Samples LW03, LW13, and LW45 were chosen for calibration studies because they cover the range of textures for our soils (i.e., LW45 and LW13 have the lowest and medium sand content, respectively, and LW03 has the lowest clay content). Comparisons were made between gravimetric soil water content and volumetric SM as determined by the TDR factory-supplied calibration. The comparisons showed that the SM values from TDR readings agree with gravimetric water contents with a determination coefficient up to 0.99, and a standard estimation error lower than ± 0.018 $\mathrm{m}^3 \cdot \mathrm{m}^{-3}$. Thus, we concluded that the effect of using the factory-supplied calibration of soil water content from the TDR readings was within its calibration uncertainty (i.e., ± 0.03 $\mathrm{m}^3 \cdot \mathrm{m}^{-3}$).

C. Emissivity Measurement: The Box Method

TIR emissivities of the soils were determined in our laboratory using the two-lid variant of the Box method, whose methodology and background were analyzed in detail by Rubio *et al.* [23], [24]. The radiance measurements were carried out with the high-precision multichannel TIR radiometer CIMEL Electronique CE-312 [25]. It has four spectral channels: one broad 8.0–13.3-μm (channel 1) and three narrow channels (channels 2–4), whose effective wavelengths (λ_{eff}) and full-width at half-maximum $(\Delta\lambda)$ are 11.96 μm (11.5–12.4 μm), 10.80 μm (10.2–11.3 μm), and 8.82 μm (8.3–9.3 μm), respectively. CE-312 was calibrated with a Landcal Blackbody Source (Type P80P) within the temperature range of -5 °C to 50 °C during our experiment, and uncertainties of about ± 0.10 K were obtained for all channels. The sensitivity analysis performed by Mira *et al.* [26] for the Box method showed that such radiometric errors yield uncertainties in emissivity of about ± 0.012, and no systematic errors.

According to the two-lid variant of the Box method, the emissivity of a sample is obtained from a sequence of measurements of radiance in which a bottomless box with specular reflective walls is used in four different configurations. Two interchangeable lids with different reflectivities were used as tops. One of them (the cold lid) has an emissivity $\varepsilon_c = 0.03$, whereas the other (the hot lid) has an emissivity $\varepsilon_h = 0.98$, and its temperature is kept 15 to 20 °C over that of the sample. A thick insulating material covers the outer walls and lids of the box to insure the thermal homogeneity of the system. For additional details on the measurement technique, the reader is referred to [24].

For each soil sample and SM value, a series of 30 emissivity measurements in each spectral channel of the radiometer was carried out. Afterward, the average value of the spectral channel emissivity of each soil and SM condition was obtained from these series. The sequence of soil saturation and drying was repeated at least two times in order to ensure the validity and reproducibility of emissivity measurements as well as to obtain intermediate values of emissivity along the SM range. For further details on the experimental setup, see [14].

III. Results and Discussion

The results of the experiment are summarized in Fig. 1, which shows the influence of soil water content on the TIR emissivity of the different samples. Notice that the lack of data for intermediate water contents of sample LW52 was due to the appearance of soil cracks on its surface during the drying process, resulting in a nondesired cavity effect contribution to the spectra. The drying process of the samples took from one to four weeks, depending on the soil texture. As expected, there is a common increase of TIR emissivities with SM. The increase is clearly larger than the standard uncertainty of the measurements, which is about ± 0.003 (Table II). The emissivity error is the estimated standard deviation of the set of 30 emissivity measurements taken for each sample, SM value, and band. Quantitatively, the highest variation of emissivity with soil water content is observed in channel 4 (8.3–9.3 μm), followed by variations in channel 1 (8.0–13.3 μm), and finally channel 2 (11.5–12.4 μm) and channel 3 (10.2–11.3 μm). A large increase of emissivity at low water content is observed in all samples, whereas there is almost no change in emissivity for moisture levels above the field capacity (FC) of the soils. FC is the water content held in soil after excess water has drained away and the drainage ceases. We conclude that soils with SM higher than its FC have thermal emissivities close to one as a result of the water spectrum, since water is retained in the soil macropores. Furthermore, below the FC point, water is retained in micropores, and macropores are full of air, allowing lower emissivity values as well as a considerable emissivity variation with SM content and spectral region. Hence, the increase of soil water content results in a sharp decrease in spectral contrast, since water is very strongly absorbing in the region of the quartz Reststrahlen bands [8].

A. Spectral Emissivity Dependence on SM: Soil-Specific Relationships

In order to quantitatively determine the behavior of TIR emissivities of bare soils with SM variation, it was decided to study which are the best relationships between both parameters. Mira *et al.* [14] found that the best fit is achieved by each particular soil following

$$\varepsilon_i = a_i + b_i\theta_v + c_i\theta_v^2 \tag{1}$$

where θ_v is the volumetric SM $(\mathrm{m}^3 \cdot \mathrm{m}^{-3})$; a, b, and c are the regression coefficients; and the subscript i represents the CE-312 channel 1, 2, 3, or 4. However, further analysis shows that there is a slight improvement when the measurements of

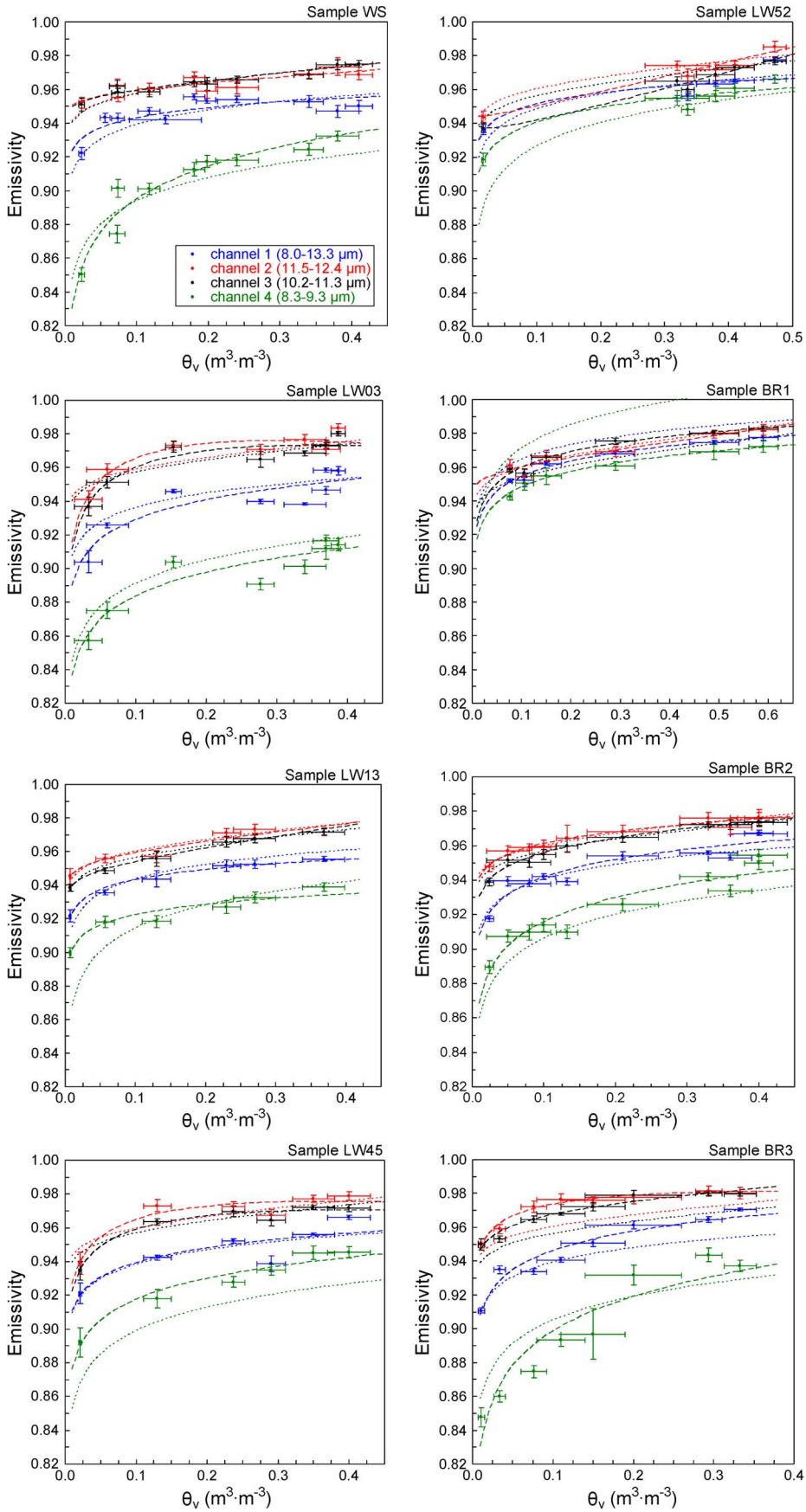

Fig. 1. Soil emissivity measurements for channel 1 (8.0–13.3 μm), channel 2 (11.5–12.4 μm), channel 3 (10.2–11.3 μm), and channel 4 (8.3–9.3 μm) of the CE-312, at various moisture contents. Dashed (dotted) lines represent the fitting regression curves of emissivity against soil water content for each channel and sample, according to (2) [(4)] and coefficients given in Table III (Table IV).

TABLE II
EMISSIVITY RANGE (I.E., DIFFERENCE BETWEEN THE HIGHEST AND THE LOWEST EMISSIVITY VALUE) WITHIN THE WHOLE SM RANGE ($\Delta\varepsilon_i$) AND ITS ERROR ($\delta(\Delta\varepsilon_i)$), AND AVERAGE OF STANDARD UNCERTAINTY OF THE MEASUREMENTS ($\overline{\delta\varepsilon_i}$), FOR EACH SAMPLE IN THE FOUR SPECTRAL CHANNELS OF CE-312

Sample	$\Delta\varepsilon_1 \pm \delta(\Delta\varepsilon_1)$	$\Delta\varepsilon_2 \pm \delta(\Delta\varepsilon_2)$	$\Delta\varepsilon_3 \pm \delta(\Delta\varepsilon_3)$	$\Delta\varepsilon_4 \pm \delta(\Delta\varepsilon_4)$	$\overline{\delta\varepsilon_1}$	$\overline{\delta\varepsilon_2}$	$\overline{\delta\varepsilon_2}$	$\overline{\delta\varepsilon_4}$
WS	0.034 ± 0.005	0.021 ± 0.008	0.024 ± 0.006	0.082 ± 0.007	0.003	0.004	0.003	0.004
LW03	0.055 ± 0.008	0.042 ± 0.008	0.043 ± 0.007	0.059 ± 0.009	0.002	0.003	0.003	0.004
LW13	0.034 ± 0.005	0.028 ± 0.008	0.033 ± 0.004	0.039 ± 0.006	0.003	0.003	0.003	0.003
LW45	0.045 ± 0.008	0.040 ± 0.009	0.037 ± 0.007	0.053 ± 0.012	0.003	0.004	0.003	0.005
LW52	0.041 ± 0.005	0.041 ± 0.006	0.040 ± 0.005	0.047 ± 0.006	0.0019	0.003	0.003	0.003
BR1	0.025 ± 0.002	0.028 ± 0.007	0.026 ± 0.004	0.030 ± 0.005	0.0016	0.003	0.0019	0.004
BR2	0.050 ± 0.003	0.028 ± 0.006	0.035 ± 0.005	0.065 ± 0.007	0.0017	0.004	0.003	0.004
BR3	0.060 ± 0.002	0.031 ± 0.005	0.030 ± 0.005	0.096 ± 0.009	0.0018	0.003	0.002	0.005

TABLE III
FITTING CURVES OF EMISSIVITY ε AGAINST VOLUMETRIC WATER CONTENT θ_v ($m^3 \cdot m^{-3}$) FOR EACH SOIL (INCLUDING A TO F FROM [14]) AND SPECTRAL BAND OF THE RADIOMETER CE-312. a, b, c: REGRESSION COEFFICIENTS; R^2: DETERMINATION COEFFICIENT; σ: STANDARD ESTIMATION ERROR

	$\varepsilon_i = a_i + b_i\,\theta_v + c_i\,ln(\theta_v)$								
	a	c	R^2	σ	a	b (m^3m^{-3})$^{-1}$	c	R^2	σ
Samples	Channel 1 (8-13 μm) b = 0 (m^3m^{-3})$^{-1}$				Channel 2 (12.0 μm)				
WS	0.963	0.009	0.66	0.006	0.963	0.02	0.003	0.75	0.004
LW03	0.968	0.017	0.80	0.009	1.03	-0.08	0.025	0.88	0.005
LW13	0.963	0.0087	0.98	0.002	0.965	0.04	0.004	0.92	0.004
LW45	0.968	0.012	0.76	0.009	1.01	-0.05	0.019	0.91	0.006
LW52	0.973	0.009	0.75	0.008	0.94	0.09	-0.001	0.95	0.004
BR1	0.9842	0.0129	0.97	0.002	0.96	0.04	0.003	0.90	0.004
BR2	0.975	0.0146	0.88	0.005	0.980	0.009	0.008	0.96	0.002
BR3	0.984	0.0165	0.93	0.006	1.005	-0.031	0.0122	0.97	0.002
A	0.9698	0.0117	0.94	0.002	1.023	-0.068	0.0253	0.99	0.0007
B	0.952	0.025	0.98	0.004	0.966	0.03	0.010	0.98	0.003
C	0.966	0.026	0.95	0.006	0.929	0.040	0.006	0.98	0.004
D	0.965	0.003	0.23	0.005	0.990	-0.023	0.0116	0.97	0.0011
E	0.987	0.0155	0.99	0.0018	0.98	0.02	0.010	0.97	0.004
F	0.991	0.020	0.79	0.005	1.18	-0.33	0.09	0.80	0.006
All samples	0.970	0.0127	0.47	0.014	0.990	-0.019	0.0114	0.62	0.007
Samples	Channel 4 (8.8 μm) b = 0 (m^3m^{-3})$^{-1}$				Channel 3 (10.8 μm)				
WS	0.960	0.028	0.92	0.008	0.963	0.034	0.003	0.92	0.002
LW03	0.930	0.020	0.85	0.009	1.02	-0.07	0.024	0.89	0.006
LW13	0.943	0.009	0.92	0.004	0.958	0.052	0.0041	0.99	0.0016
LW45	0.959	0.0179	0.96	0.005	1.004	-0.04	0.018	0.97	0.003
LW52	0.97	0.0127	0.93	0.005	0.925	0.11	-0.003	0.97	0.003
BR1	0.9787	0.0134	0.98	0.0017	0.992	0.00	0.014	0.96	0.003
BR2	0.963	0.020	0.90	0.007	0.979	0.013	0.010	0.98	0.002
BR3	0.966	0.030	0.88	0.014	0.984	0.02	0.008	0.96	0.003
A	0.974	0.0184	0.96	0.003	0.996	-0.034	0.016	0.90	0.002
B	0.916	0.053	0.96	0.014	0.959	0.03	0.008	0.97	0.004
C	0.963	0.026	0.93	0.007	0.928	0.041	0.010	0.98	0.005
D	0.967	0.0070	0.83	0.003	0.970	-0.001	0.004	0.65	0.003
E	0.984	0.0198	0.99	0.003	0.97	0.03	0.009	0.98	0.004
F	0.999	0.028	0.89	0.005	1.08	-0.16	0.05	0.82	0.005
All samples	0.965	0.024	0.36	0.03	0.987	-0.016	0.0116	0.66	0.007

each particular soil are fitted to a logarithmic dependence on SM following

$$\varepsilon_i = a_i + b_i\theta_v + c_i \ln(\theta_v). \tag{2}$$

Fig. 1 shows the regression curves determined by (2), and Table III gives the set of regression coefficients (a, b, c), the determination coefficient (R^2), and the standard estimation error (σ) for each soil and spectral channel. In this case, the standard estimation error (σ) for each soil and spectral channel was computed as

$$\sigma = \sqrt{\frac{1}{N-2}\sum\left(a_i + b_i\theta_v + c_i \ln(\theta_v) - \varepsilon_i\right)^2} \tag{3}$$

where N is the number of values considered to obtain the fitting curves; i is the spectral channel; a, b, and c are the regression

coefficients given in Table III; and θ_v and ε are the SM and emissivity values measured at the laboratory. An equivalent formula is applied to obtain the standard estimation error (σ) from the other equations. Results for the six soils formerly studied by Mira *et al.* [14] (labeled as A to F) are also included in order to present here a more complete database with the best relationships for a wide range of soils of different textures. It is worth noting that gravimetric water contents measured by Mira *et al.* [14] were converted to volumetric SM by considering the bulk density of the soils. As detailed in [14], bulk densities were calculated following the method described in [27] or [28]. Note also that channels 1 and 4 do not depend on θ_v but only on $\ln(\theta_v)$ (see Table III). Furthermore, since the minimum SM value is at the least 0.001 $\mathrm{m}^3 \cdot \mathrm{m}^{-3}$ (residual water content), even in the case of hyperarid desert regions, the logarithmic function in (2) should not present divergence problems. It is seen that the average values from about 0.83 to 0.92 and from ± 0.003 to ± 0.006 are obtained for R^2 and σ, respectively, considering all samples of a band. According to the study in [14], an emissivity variation of ± 0.006 causes an error of ± 0.2 K in the LST determination (at 11 μm and for an LST of about 300 K). Since σ is derived from this relationship, it will be larger when the SM retrievals are less accurate (i.e., satellite SM retrievals).

B. General Dependence of Spectral Emissivities on SM and Other Soil Properties

With the aim of improving the applicability of the study, it is of great interest to find a general relationship that explains how TIR emissivities of soils with any soil texture change with SM content. Soils studied by Mira *et al.* [14] were included in the study, completing the set of samples to a total of 14 different soils and thus being a more general relationship. Soil samples analyzed in [14] contain carbonate (content up to 46%), while the samples studied here do not present carbonate content at all. If it is assumed that no knowledge is available about the soil type, except its SM, the best results are again obtained with (2), with R^2 ranging from 0.36 to 0.66 and σ from 0.007 to 0.03. These uncertainties lead to LST errors up to ± 1.1 K (at 11 μm and for an LST of about 300 K [14]). The results are summarized in Table III, and Fig. 2 shows the plots for the wide band (channel 1) and 8.82-μm band (channel 4).

To improve the predictability, a more complex relationship has to be considered which includes other parameters that influence the emissivity spectrum such as soil composition or particle size. A statistical analysis of our data was performed to determine these additional soil parameters, which should be included in our model. Three soil components were selected to be considered as inputs in the relationships. The first component is the OM content, which is highly absorbing in the 8–14-μm region and reduces the apparent spectral contrast of the quartz Reststrahlen bands. According to Salisbury and D'Aria [8], soils that contain more than 1.5%–2% extractable OM tend to display low emissivity ratios between 8.3- and 11.3-μm bands, regardless of the particle size. The second component is the quartz content, which exhibits fundamental molecular absorption features in the TIR: It increases the reflectance

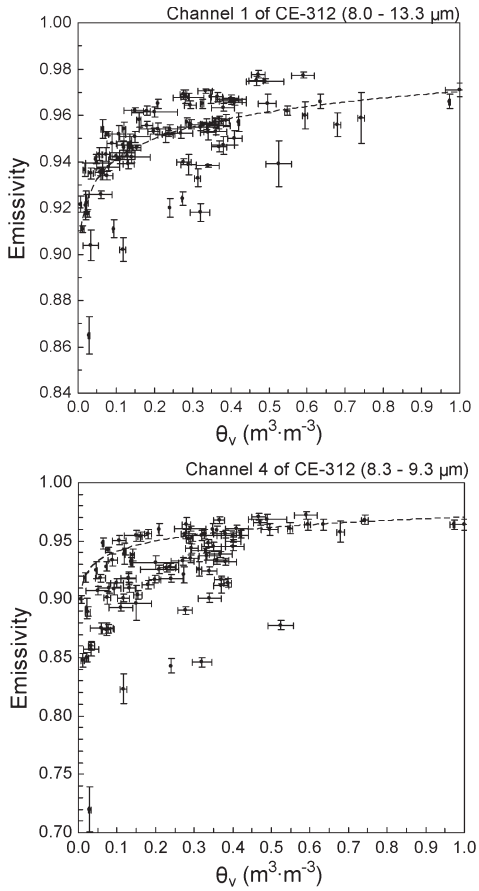

Fig. 2. Soil emissivity measurements for channel 1 (8.0–13.3 μm) and channel 4 (8.3–9.3 μm) of the CE-312, at various moisture contents. Dashed lines represent the fitting regression curves of emissivity against soil water content for all soils together, including samples from [14], and for each channel and sample, according to (2) and coefficients given in Table III.

of the material and decreases the emissivity between 7.7 and 9.7 μm, and near 12.6 μm, due to the weak absorption feature of the quartz Reststrahlen bands [4]. The third component is carbonate content, whose spectrum is distinctive because of the presence of a weak absorption feature centered near 11.2 μm and otherwise generally flat spectra [4]. Both quartz and carbonate content data improve the estimate of the 8.82-μm-band (channel 4) and the wide-band (channel 1) emissivities. However, they are not essential for emissivity estimates at 11.96 μm (channel 2) and 10.80 μm (channel 3). The regression relationship presenting the best results for each band when considering not only SM but also OM, quartz (Q), and carbonate (C) contents is

$$\varepsilon_i = a_i + b_i\theta_v + c_i \ln(\theta_v) + d_i OM + e_i OM^2 + f_i Q + g_i C \tag{4}$$

where a to g are the regression coefficients for each spectral channel i ($i = 1$ to 4) and OM, Q, and C contents are given in percentage. The results of this analysis are summarized in Table IV, and Fig. 1 shows the regression curves for each soil. Note that the regression curve resulting for channel 4 of sample BR1 does not fit very well the measured values, which could be due to the underestimation (overestimation) of its quartz (OM) content. As in the case of (2), the logarithmic function in (4)

TABLE IV
FITTING CURVES OF EMISSIVITY ε AGAINST VOLUMETRIC WATER CONTENT θ_v ($m^3 \cdot m^{-3}$) AND OTHER SOIL PROPERTIES, FOR EACH SPECTRAL BAND OF CE-312, WHEN CONSIDERING ALL SOILS TOGETHER, INCLUDING SAMPLES FROM [14]. OM: ORGANIC MATTER CONTENT (%); Q: QUARTZ CONTENT (%); C: CARBONATE CONTENT (%); a TO g: REGRESSION COEFFICIENTS; R^2: DETERMINATION COEFFICIENT; σ: STANDARD ESTIMATION ERROR

	$\varepsilon_i = a_i + b_i\theta_v + c_i\, ln(\theta_v) + d_i OM + e_i OM^2 + f_i Q + g_i C$			
	Channel 1 (8-13 μm)	Channel 2 (12.0 μm)	Channel 3 (10.8 μm)	Channel 4 (8.8 μm)
a ± δ (a)	0.964 ± 0.003	0.968 ± 0.004	0.970 ± 0.004	0.930 ± 0.007
b ± δ (b), $(m^3m^{-3})^{-1}$	0	0.027 ± 0.007	0.025 ± 0.007	0
c ± δ (c)	0.0124 ± 0.0010	0.0060 ± 0.0013	0.0065 ± 0.0013	0.020 ± 0.002
d ± δ (d)	0.0186 ± 0.0019	0.0033 ± 0.0009	0	0.050 ± 0.004
e ± δ (e)	-0.00198 ± 0.00019	-0.00078 ± 0.00011	-0.00045 ± 0.00004	-0.0047 ± 0.0004
f ± δ (f)	-0.00022 ± 0.00004	0	0	-0.0005 ± 0.00008
g ± δ (g)	-0.00052 ± 0.00010	0	0	-0.0013 ± 0.0002
R^2	0.77	0.79	0.77	0.79
σ	0.009	0.006	0.006	0.019

should not present divergence problems since the minimum SM value is at least 0.001 $m^3 \cdot m^{-3}$. As expected, the consideration of ancillary data in relationship (2) significantly improved the emissivity estimation (see Tables III and IV for comparisons). Quantitatively, R^2 took an average value of 0.78, and σ was lower than ± 0.019, leading to LST errors lower than ± 0.7 K (at 11 μm and for an LST of about 300 K [14]). Here, σ represents the minimum achievable error, which will be larger as far as the parameters' estimation (i.e., θ_v, OM, Q, and C) becomes less accurate. We consider that such an emissivity approach is quite satisfactory, despite the fact that quantities of other minerals (i.e., feldspars, magnetite, or hematite) have not been taken into account.

If (4) were to be applied to remote sensing observations, the OM, quartz, and carbonate contents would be estimated using visible/infrared data. As shown in [9], quartz and carbonate contents can be derived by means of spectral indices for lithologic mapping with TIR data from the Advanced Spaceborne Thermal Emission and Reflection radiometer (ASTER). Quartz minerals can be detected using bands 10 (8.3 μm), 11 (8.6 μm), and 12 (9.1 μm), and carbonates can be detected using bands 13 (10.7 μm) and 14 (11.3 μm). According to the study in [9], the result of applying the indices to level 1B ASTER TIR data sets observing a study site at various seasons indicates that they are robust against variations in atmospheric conditions and surface temperatures. Other approach to estimate the carbonate content in a soil was proposed in [29] and [30] by using airborne hyperspectral measurements. A continuum removal technique quantifying specific absorption features of carbonate (2.341 μm) was applied to HYMAP reflectance measurements. Regarding OM content, it can be estimated from Landsat Enhanced Thematic Mapper (ETM) bands 2 (0.52–0.60 μm) and 7 (2.08–2.35 μm) following a regression equation with a coefficient of correlation $R^2 = 0.51$ [10]. Frazier and Cheng [31] obtained $R^2 = 0.98$ for predictive OM equations, using the ratio between the ETM's bands 5 (1.55–1.75 μm) and 4 (0.76–0.90 μm). Wu *et al.* [32] found that the highest correlation ($R^2 = 0.59$) between OM of 131 soil samples and the corresponding digital number of ETM reflective bands was with band 1 (0.45–0.52 μm).

C. SM Retrieval From TIR Emissivities

A complementary result was considered in this paper, i.e., the possibility of retrieving soil water content from TIR emissivity estimates. Keeping in mind the previous inverse model (i.e., (2) and Table III) and avoiding redundancy by considering variables presenting the same dependence (i.e., ε_1 and ε_4, ε_2 and ε_3), emissivities in channel 3 (10.80 μm) and channel 4 (8.82 μm) were selected as the most representatives to explain the SM content in terms of TIR emissivities. Hence, a statistical analysis showed that the best estimates of SM were retrieved by the following relationship:

$$\theta_v = A + B\exp(\varepsilon_3) + C\exp(\varepsilon_4) + D(\varepsilon_4)^2 + E(\varepsilon_3\varepsilon_4) + F(\varepsilon_3\varepsilon_4)^2 \quad (5)$$

where A to F are the regression coefficients and ε_i is the emissivity of channel $i (i = 3, 4)$ of the CE-312 radiometer. The results of the analysis, summarized in Table V-I, showed that R^2 was about 0.61, being the standard estimation error (σ) of SM of about ± 0.11 $m^3 \cdot m^{-3}$, which can be larger if emissivity estimates are less accurate. When the inclusion of ancillary data was carried out, the best estimates of SM were obtained following

$$\theta_v = A + B\exp(\varepsilon_3) + C\exp(\varepsilon_4) + D(\varepsilon_4) + E\,OM + F(OM)^2. \quad (6)$$

Quartz and carbonate contents were not included in the model since they do not imply a significant improvement on the SM estimation. In this case, R^2 improved to 0.85 and σ to ± 0.08 $m^3 \cdot m^{-3}$ (Table V-II). Therefore, this approach could be considered as a way to roughly estimate SM when the emissivity spectrum and OM content of the soil are known. As aforementioned, if (6) were to be applied to remote sensing observations, the OM content would be estimated using visible/infrared data [10], [31], [32]. Then, the advantage of this method with respect to SM retrievals from microwave-based sensors is the possibility of working with a higher spatial

TABLE V
FITTING CURVES OF VOLUMETRIC WATER CONTENT θ_v ($m^3 \cdot m^{-3}$) AGAINST TIR EMISSIVITIES OF CHANNEL 3 (10.80 μm) AND CHANNEL 4 (8.82 μm) **(I)** AND OM CONTENT **(II)**, WHEN CONSIDERING ALL SOILS TOGETHER (INCLUDING SAMPLES FROM [14]). A TO F: REGRESSION COEFFICIENTS ($m^3 \cdot m^{-3}$); R^2: DETERMINATION COEFFICIENT; σ: STANDARD ESTIMATION ERROR ($m^3 \cdot m^{-3}$)

I $\theta_v = A + B\exp(\varepsilon_3) + C\exp(\varepsilon_4) + D(\varepsilon_4)^2 + E(\varepsilon_3\ \varepsilon_4) + F(\varepsilon_3\ \varepsilon_4)^2$	
A ± δ(A)	-851 ± 17
B ± δ(B)	68 ± 15
C ± δ(C)	580 ± 120
D ± δ(D)	-690 ± 150
E ± δ(E)	-260 ± 50
F ± δ(F)	41 ± 13
R^2	0.61
σ	0.11
II $\theta_v = A + B\exp(\varepsilon_3) + C\exp(\varepsilon_4) + D(\varepsilon_4) + E\ OM + F(OM)^2$	
A ± δ(A)	-15.4 ± 1.2
B ± δ(B)	2.8 ± 0.3
C ± δ(C)	29 ± 5
D ± δ(D)	-70 ± 12
E ± δ(E)	-0.113 ± 0.018
F ± δ(F)	0.0166 ± 0.0017
R^2	0.85
σ	0.08

resolution, while the disadvantages are the loss of precision in the SM retrievals and the fact that only soil water content from the skin of the surface can be retrieved by TIR remote sensing. Furthermore, the near-surface moisture content has a short lifetime, and clear sky conditions are required for TIR emissivity retrievals. Nevertheless, it would be useful to compare the results with future SM missions such as the European Spatial Agency's Soil Moisture and Ocean Salinity (SMOS) [33] and the National Aeronautics and Space Administration (NASA)'s Soil Moisture Active and Passive [34].

IV. SUMMARY AND CONCLUSIONS

TIR emissivities of soils with different textures were measured for a wide range of controlled SM contents in order to obtain quantitative relationships between SM and spectral emissivities. Thermal emissivities were determined at the laboratory using the two-lid variant of the Box method [24], with an expected uncertainty of about ±0.003. The radiances were measured using a high-precision multichannel TIR radiometer CIMEL Electronique CE-312 with ±0.10 K of uncertainty [25]. Soil water contents were determined by using the factory-supplied calibration from TDR readings of the Delta-T SM200 sensor, which has a calibration uncertainty of ±0.03 $m^3 \cdot m^{-3}$ [22].

As reported by previous studies, there is a common increase of emissivity with SM. This increase is more apparent in the 8–9-μm range for sandy soils due to the presence of either quartz or gypsum, while the 10–12-μm channels show little variation with either soil type or SM. Furthermore, a large increase of emissivity is observed at low water contents, while there is almost no change in emissivity for moisture levels above the soil FC. Hence, the highest emissivity variations are observed in sandy soils, particularly in the 8–9-μm range, due to water adhering to soil grains and decreasing the reflectance in the 8–9-μm region.

Since the scope of the study was to model emissivity dependence on soil water content, different approaches were presented, according to the *a priori* information about the soil. When a specific retrieval procedure was applied to each soil, the standard estimation error of retrieved emissivities from volumetric SM was better than ±0.014 for any channel and soil. When a general retrieval procedure was applied, regardless of the soil type, rough estimates of the emissivities were retrieved with a standard estimation error from ±0.007 to ±0.03. However, the study also indicated that the consideration of ancillary data (i.e., OM, quartz, and carbonate contents) significantly improved the results from a general fitting curve applicable to any soil, providing the emissivity with a standard estimation error lower than ±0.019. Furthermore, the possibility of retrieving soil water content from emissivity estimates was also analyzed. SM was obtained with a standard estimation error of about ±0.11 $m^3 \cdot m^{-3}$, or ±0.08 $m^3 \cdot m^{-3}$ when OM content was considered. This could be obtained when the TIR emissivity spectrum can be measured with high precision and no data of soil water content are available or it has a poor spatial resolution.

The results are moderately satisfying and encouraging because the data sets used included a large range of SM and soil textures. In addition, the uncertainty in surface temperature associated with such emissivity errors took values of about ±0.2 K and ±1.1 K (at 11 μm and for an LST of about 300 K [14]) from the specific and general relationships, respectively. An important feature of the retrieval relationships is that if the soil composition is known, accurate retrievals of TIR emissivities from SM are possible.

This study, which includes data from [14], provides the first database on SM effects on emissivity. Thus, this work could be used to estimate thermal emissivities of moist soils with a wide variety of textures, which has been difficult up to now due to the lack of published data. Emissivity maps or time series analysis of emissivities retrieved from both current LST and emissivity radiance-based retrieval algorithms (e.g., Moderate Resolution Imaging Spectroradiometer (MODIS) day/night [35] and ASTER TES [1]) could be improved by this study since it explains emissivity deviation errors due to the sensitivity of TIR emissivities of bare soils on SM. Land surface emissivity estimation from SM might be useful to better understand emissivity variations from ASTER and MODIS over bare and semiarid areas. Furthermore, this work could help to discriminate between land surface emissivity variations (from MODIS and ASTER retrievals) caused by atmospheric correction effects and SM effects. According to the approach presented in Section III-C, emissivity retrievals from ASTER and MODIS will allow to estimate SM contents. Therefore, in

further work, we will explore the feasibility of this approach using SMOS data and compare the retrieved emissivities with those coming from other sources, e.g., emissivities from the MODIS and the ASTER sensors onboard the NASA's Terra satellite.

ACKNOWLEDGMENT

The authors would like to thank Dr. T. Schmugge from New Mexico State University for assisting them with fieldwork at White Sands, CLASIC07 field campaign in Oklahoma for providing them with four soil samples from LWREW, and Dr. S. Rolim from the Federal University of Rio Grande do Sul for her helpful comments on mineralogy. The authors would also like to thank the two anonymous referees who have brought valuable comments and suggestions that helped improve this paper.

REFERENCES

[1] A. Gillespie, S. Rokugawa, T. Matsunaga, J. S. Cothern, S. Hook, and A. B. Kahle, "A temperature and emissivity separation algorithm for Advanced Spaceborne Thermal Emission and Reflection Radiometer (ASTER) images," *IEEE Trans. Geosci. Remote Sens.*, vol. 36, no. 4, pp. 1113–1126, Jul./Aug. 1998.

[2] Y. Yu, J. P. Privette, and A. C. Pinheiro, "Evaluation of split window land surface temperature algorithms for generating climate data records," *IEEE Trans. Geosci. Remote Sens.*, vol. 46, no. 1, pp. 179–192, Jan. 2008.

[3] J. M. Galve, C. Coll, V. Caselles, and E. Valor, "An Atmospheric Radiosounding database for generating land surface temperature algorithms," *IEEE Trans. Geosci. Remote Sens.*, vol. 46, no. 5, pp. 1547–1557, May 2008.

[4] L. C. Rowan and J. C. Mars, "Lithologic mapping in the Mountain Pass, California area using Advanced Spaceborne Thermal Emission and Reflection radiometer (ASTER) data," *Remote Sens. Environ.*, vol. 84, no. 3, pp. 350–366, Mar. 2002.

[5] R. G. Vaughan, S. J. Hook, W. M. Calvin, and J. V. Taranik, "Surface mineral mapping at Steamboat Springs, Nevada, USA, with multiwavelength thermal infrared images," *Remote Sens. Environ.*, vol. 99, no. 1/2, pp. 140–158, Nov. 2005.

[6] I. F. Trigo, L. F. Peres, C. C. DaCamara, and S. C. Freitas, "Thermal land surface emissivity retrieved from SEVIRI/Meteosat," *IEEE Trans. Geosci. Remote Sens.*, vol. 46, no. 2, pp. 307–314, Feb. 2008.

[7] K. Ogawa, T. Schmugge, and S. Rokugawa, "Estimating broadband emissivity of arid regions and its seasonal variations using thermal infrared remote sensing," *IEEE Trans. Geosci. Remote Sens.*, vol. 46, no. 2, pp. 334–343, Feb. 2008.

[8] J. W. Salisbury and D. M. D'Aria, "Infrared (8–14 μm) remote sensing of soil particle size," *Remote Sens. Environ.*, vol. 42, no. 2, pp. 157–165, Nov. 1992.

[9] Y. Ninomiya and B. Fu, "Spectral indices for lithologic mapping with ASTER thermal infrared data applying to a part of Beishan Mountains, Gansu, China," in *Proc. IEEE Int. Geosci. Remote Sens. Symp.*, 2001, vol. 7, pp. 2988–2990.

[10] M. R. Nanni and J. A. Demattê, "Spectral reflectance methodology in comparison to traditional soil analysis," *Soil Sci. Soc. Amer.*, vol. 70, no. 2, pp. 393–407, Mar./Apr. 2006.

[11] M. Urai, T. Matsunaga, and T. Ishii, "Relationship between soil moisture content and thermal infrared emissivity of the sand sampled in Muus Desert, China," *Remote Sens. Soc. Jpn.*, vol. 17, no. 4, pp. 322–331, 1997.

[12] Q. Xiao, Q. H. Liu, X. W. Li, L. F. Chen, Q. Liu, and X. Z. Xin, "A field measurement method of spectral emissivity and research on the feature of soil thermal infrared emissivity," *J. Infrared Millim. Waves*, vol. 22, no. 5, pp. 373–378, 2003.

[13] K. Ogawa, T. J. Schmugge, and S. Rokugawa, "Observations of the dependence of the thermal infrared emissivity on soil moisture," *Geophys. Res. Abstracts*, vol. 8, p. 04 996, 2006.

[14] M. Mira, E. Valor, R. Boluda, V. Caselles, and C. Coll, "Influence of soil water content on the thermal infrared emissivity of bare soils: Implication for land surface temperature determination," *J. Geophys. Res.*, vol. 112, no. F4, p. F04 003, 2007, DOI:10.1029/2007JF000749.

[15] C. Warshall and R. Roy, "Classification and scheme for the identification of layer silicates," *Geol. Soc. Amer. Bull.*, vol. 72, pp. 1455–1492, 1961.

[16] B. L. Davis and D. Smith, "Table of experimental reference intensity ratios," *Powder Diffr.*, vol. 3, pp. 201–205, 1989.

[17] B. L. Davis and D. Smith, "Table of experimental reference intensity ratios. Table n° 2," *Powder Diffr.*, vol. 4, pp. 206–209, 1989.

[18] G. C. Topp, J. L. Davis, and A. P. Annan, "Electromagnetic determination of soil water content: Measurements in coaxial transmission lines," *Water Resour. Res.*, vol. 16, no. 3, pp. 574–582, 1980.

[19] G. C. Topp and W. D. Reynolds, "Time domain reflectometry: A seminal technique for measuring mass and energy in soil," *Soil Till. Res.*, vol. 47, no. 1/2, pp. 125–132, Jun. 1998.

[20] C. H. Roth, M. A. Malicki, and R. Plagge, "Empirical evaluation of the relationship between soil dielectric constant and volumetric water content as the basis for calibrating soil moisture measurement," *J. Soil Sci.*, vol. 43, no. 1, pp. 1–13, Mar. 1992.

[21] A. Malicki, R. Plagge, and C. H. Roth, "Improving the calibration of dielectric TDR soil moisture determination taking into account the solid soil," *Eur. J. Soil Sci.*, vol. 47, no. 3, pp. 357–366, Sep. 1996.

[22] *User Manual for the SM200 Soil Moisture Sensor*, Delta-T Devices Ltd., Cambridge, U.K., May 2006, p. 3.6, SM200-UM-1.1.

[23] E. Rubio, V. Caselles, and C. Badenas, "Emissivity measurements of several soils and vegetation types in the 8–14 μm wave band: Analysis of two field methods," *Remote Sens. Environ.*, vol. 59, no. 3, pp. 490–521, Mar. 1997.

[24] E. Rubio, V. Caselles, C. Coll, E. Valor, and F. Sospedra, "Thermal-infrared emissivities of natural surfaces: Improvements on the experimental set-up and new measurements," *Int. J. Remote Sens.*, vol. 24, no. 24, pp. 5379–5390, 2003.

[25] G. Brogniez, C. Pietras, M. Legrand, P. Dubuisson, and M. Haeffelin, "A high-accuracy multiwavelength radiometer for *in situ* measurements in the thermal infrared—Part II: Behavior in field experiments," *J. Atmos. Ocean Technol.*, vol. 20, no. 7, pp. 1023–1033, Jul. 2003.

[26] M. Mira, T. J. Schmugge, E. Valor, V. Caselles, and C. Coll, "Comparison of thermal infrared emissivities retrieved with the two-lid Box and the TES methods with laboratory spectra," *IEEE Trans. Geosci. Remote Sens.*, vol. 47, no. 4, pp. 1012–1021, Apr. 2009.

[27] K. E. Saxton, W. J. Rawls, J. S. Romberger, and R. I. Papendick, "Estimating generalized soil-water characteristics from texture," *Soil Sci. Soc. Amer. J.*, vol. 50, no. 4, pp. 1031–1036, Jul. 1986.

[28] M. D. Soriano and V. Pons, *Prácticas de Edafología y Climatología*. Valencia, Spain: Univ. Politècnica de València, 2001.

[29] J. M. Netto, J. M. Robbez-Masson, and E. Martins, "Visible-NIR hyperspectral imagery for discriminating soil types in the La Peyne watershed (France)," in *Proc. Digital Soil Mapping*, Montpellier, France, 2006.

[30] P. Lagacherie, F. Baret, J.-B. Feret, J. M. Netto, and J. M. Robbez-Masson, "Estimation of soil clay and calcium carbonate using laboratory, field and airborne hyperspectral measurements," *Remote Sens. Environ.*, vol. 112, no. 3, pp. 825–835, Mar. 2008.

[31] B. E. Frazier and Y. Cheng, "Remote sensing of soils in the eastern Palouse region with Landsat Thematic Mapper," *Remote Sens. Environ.*, vol. 28, pp. 317–325, Apr./Jun. 1989.

[32] C. Wu, J. Wu, Y. Luo, L. Zhang, and S. D. DeGloria, "Spatial prediction of soil organic matter content using cokriging with remotely sensed data," *Soil Sci. Soc. Amer. J.*, vol. 73, no. 4, pp. 1202–1208, Jul./Aug. 2009.

[33] Y. H. Kerr, P. Waldteufel, J.-P. Wigneron, J.-M. Martinuzzi, J. Font, and M. Berger, "Soil moisture retrieval from space: the Soil Moisture and Ocean Salinity (SMOS) mission," *IEEE Trans. Geosci. Remote Sens.*, vol. 39, no. 8, pp. 1729–1735, Aug. 2001.

[34] D. Entekhabi, E. G. Njoku, P. Houser, M. Spencer, T. Doiron, Y. J. Kim, J. Smith, R. Girard, S. Belair, W. Crow, T. J. Jackson, Y. H. Kerr, J. S. Kimball, R. Koster, K. C. McDonald, P. E. O'Neill, T. Pultz, S. W. Running, J. C. Shi, E. Wood, and J. van Zyl, "The Hydrosphere State (Hydros) satellite mission: An earth system pathfinder for global mapping of soil moisture and land freeze/thaw," *IEEE Trans. Geosci. Remote Sens.*, vol. 42, no. 10, pp. 2184–2195, Oct. 2004.

[35] Z. Wan and Z. L. Li, "A physics-based algorithm for retrieving landsurface emissivity and temperature from EOS/MODIS data," *IEEE Trans. Geosci. Remote Sens.*, vol. 35, no. 4, pp. 980–996, Jul. 1997.

[36] K. E. Saxton and W. J. Rawls, "Soil water characteristic estimates by texture and organic matter for hydrologic solutions," *Soil Sci. Soc. Amer. J.*, vol. 70, no. 5, pp. 1569–1578, Sep./Oct. 2006.

Maria Mira was born in Ontinyent, Spain, in 1982. She received the B.Sc. degree (first-class honors) in physics and the M.Sc. degree in environmental physics and thermodynamics from the University of Valencia, Burjassot, Spain, in 2005 and 2007, respectively, where she is currently working toward the Ph.D. degree in physics.

From December 2007 to March 2008, she was a Visiting Student with New Mexico State University, Las Cruces. From September to December 2009, she was with INRA-Bordeaux, France. Her research interest focuses on the physical processes of thermal infrared remote sensing, including the retrieval of surface emissivity from thermal infrared remotely sensed data supplied by the Moderate Resolution Imaging Spectroradiometer and the Advanced Spaceborne Thermal Emission and Reflection Radiometer sensors, as well as by field radiometers.

Enric Valor received the B.Sc., M.Sc., and Ph.D. degrees in physics from the University of Valencia, Burjassot, Spain, in 1992, 1994, and 1997, respectively.

He is currently an Associate Professor of earth physics with the Department of Earth Physics and Thermodynamics, Faculty of Physics, University of Valencia. He has published 35 papers in international journals and 45 conference papers. His research interest focuses on the physical processes of thermal infrared remote sensing, emissivity measurement and characterization, atmospheric and emissivity corrections, and temperature emissivity separation algorithms.

Vicente Caselles received the B.Sc., M.Sc., and Ph.D. degrees in physics from the University of Valencia, Burjassot, Spain, in 1979, 1980, and 1983, respectively.

He is currently a Professor in applied physics and the Head of the Thermal Remote Sensing Group, Department of Earth Physics and Thermodynamics, Faculty of Physics, University of Valencia. He has 32 years expertise in the physical processes involved in both temperature measurement and evapotranspiration using remote sensing techniques, which has been documented through 10 books, 20 doctoral theses, 100 papers in international journals, 60 conference papers, and 30 reports. He was collaborating with the European Space Agency as a member of the Advisory Group for the Land-Surface Processes and Interactions Mission. He was the Chairman of the Spanish Remote Sensing Society and is currently the Manager of Human Resources and Researchers Mobility General Direction at the Spanish Ministry of Science and Innovation.

Dr. Caselles received the Norbert Gerbier–MUMM International Award for 2010, conferred by the Executive Council of the World Meteorological Organization.

Eva Rubio received the B.Sc., M.Sc., and Ph.D. degrees in physics from the University of Valencia, Burjassot, Spain, in 1993, 1994, and 1998, respectively.

She is currently an Assistant Professor of physics with the Department of Applied Physics, School of Industrial Engineering of Albacete, University of Castilla-La Mancha (UCLM), Albacete, Spain, and a Senior Researcher with the Remote Sensing and G.I.S. Unit, Institute of Regional Development, UCLM. She has published more than 20 papers in peer-reviewed journals. Her research interests include thermal infrared remote sensing, in particular emissivity measurement and atmospheric and emissivity correction techniques, and physics of land surface processes (energy, water, and CO_2 balances).

César Coll received the B.Sc., M.Sc., and Ph.D. degrees in physics from the University of Valencia, Burjassot, Spain, in 1989, 1992, and 1994, respectively.

He is currently an Associate Professor of earth physics with the Department of Earth Physics and Thermodynamics, Faculty of Physics, University of Valencia. He has published 40 papers in international journals and 50 conference papers. His research interest focuses on the physical processes of thermal infrared (TIR) remote sensing, atmospheric and emissivity corrections, temperature emissivity separation, and ground validation of Advanced Along Track Scanning Radiometer, Moderate Resolution Imaging Spectroradiometer, and Advance Spaceborne Thermal Emission and Reflection Radiometer TIR products.

Joan M. Galve was born in Benifaio, Spain, in July 1978. He received the B.Sc. degree in physics and the M.Sc. degree in earth physics and thermodynamics from the University of Valencia, Burjassot, Spain, in 2004 and 2006, respectively, where he is currently working toward the Ph.D. degree in physics in the Department of Earth Physics and Thermodynamics, Faculty of Physics.

His research includes the derivation and validation of land-surface temperatures from remote sensing sensors in thermal infrared.

Raquel Niclòs received the B.Sc., M.Sc., and Ph.D. degrees in physics from the University of Valencia, Burjassot, Spain, in 2000, 2002, and 2005, respectively.

She is currently a Senior Researcher with the Meteorology-Climatology Department, Mediterranean Centre for Environmental Studies (Fundación Centro de Estudios Ambientales del Mediterráneo, CEAM), Paterna, Spain. Her research is focused on sea and land remote sensing techniques, mainly related to the determination of surface temperature and thermal infrared emissivity, for environmental and meteorological applications. She has published 15 papers in international journals and more than 60 works as conference proceedings, book chapters, and national papers.

Juan M. Sánchez received the B.Sc., M.Sc., and Ph.D. degrees in physics from the University of Valencia, Burjassot, Spain, in 2003, 2005, and 2008, respectively.

He is currently a Postdoctoral Researcher with the Department of Applied Physics, School of Industrial Engineering of Albacete, University of Castilla-La Mancha, Albacete, Spain. He is also currently with the Department of Earth Physics and Thermodynamics, Faculty of Physics, University of Valencia. His research interest focuses on thermal infrared remote sensing in general and surface-energy-flux retrieval in particular, specifically on evapotranspiration estimation from two-source models and radiometric temperatures. He has published 15 papers in international journals, two book chapters, and more than 30 conference papers.

Rafael Boluda received the B.Sc., M.Sc., and Ph.D. degrees in pharmacy from the University of Valencia, Burjassot, Spain, in 1981, 1982, and 1988, respectively.

From 1983 to 1990, he was an Assistant Professor of geology and pedology with the University of Valencia. From 1990 to 2007, he was with the Soil Sciences Branch, Department of Vegetal Biology, University of Valencia. He is currently a Professor of pedology and agricultural chemistry with the Department of Vegetal Biology, where he is also Responsible of the Soils, Wastes and Environment Research Unit. He has published more than 110 national and international works on the application of environmental soil science and supervised seven doctoral theses. His research interests include the assessment of soil degradation using remote sensing techniques.